14

INJURY BIOMECHANICS RESEARCH
Proceedings of the Thirty-Third International Workshop

Mechanical Characterization of Costal Cartilage

M. L. Oyen, D. Murakami, and R. W. Kent

*This paper has not been screened for accuracy nor refereed by any body of scientific peers
and should not be referenced in the open literature.*

ABSTRACT

Rib fractures are a common morbidity following automotive crashes. While the rib bones are well-characterized, and articular cartilage from joints such as the knee and shoulder has been extensively mechanically characterized, almost no mechanical examination has been performed of the rib-cage costal cartilage. Costal cartilage is a hyaline cartilage, like articular cartilage, but it differs from articular cartilage in both structure and composition. In addition, the costal cartilage undergoes a transformation with aging, the "amianthoid change", in which the tissue becomes more tendon-like: the collagen fibrils become larger and more aligned, while the proteoglycan content is depleted. The costal cartilage can also calcify, leading to dramatic mechanical stiffening. A decrease in the mechanical compliance of aging costal cartilage, in conjunction with a decrease in bone stiffness, represents an important factor potentially associated with the increased incidence of rib fractures in elderly persons.

The current study incorporates in vitro examination of the mechanical behavior of costal cartilage in conjunction with a finite element modeling study. Experimental data will be presented for young porcine costal cartilage and for tissue from adult human cadavers of different ages. Mechanical testing is performed using an indentation methodology to allow for localized probing of tissue properties, including elastic and time-dependent behavior. Examination of costal cartilage includes characterization of both the perichondrium surface layer and of the bulk cartilage properties. Mechanical property results from costal cartilage tissue are used as input for finite element simulations examining changes in the thorax response to automotive injury with aging. The information obtained in the current study has direct relevance to the development of both physical and computational surrogates for the aging thorax.

INTRODUCTION

Older drivers are more likely than younger drivers to die of a chest injury, and less likely than younger drivers to die of a head injury (Kent et al., 2005a). Rib fractures are the most common skeletal thoracic injury sustained by restrained occupants in frontal crashes (Pattimore et al., 1992). Recent studies have considered material-level characterization of rib bone tissue (Stitzel et al., 2003; Kemper et al., 2005) although it has been shown that changes to bone properties with aging are structural, including increased porosity, and not material property changes at the tissue level (Hoffler et al., 2000). Recent research has thus focused on age-related changes to rib cage geometry (Kent et al., 2005b).

One potentially important factor in ribcage deformation is the mechanical behavior of the costal cartilage linking the rib bones to the sternum. Like articular cartilage, costal cartilage is a hyaline cartilage tissue. Although articular cartilage has been extensively characterized, there has been little mechanical examination of the ribcage costal cartilage although its composition and structure are known (Rosenburg et al., 1965; Hukins et al., 1976; Mallinger and Stockinger, 1988), as are the differences between its microstructure and that of articular cartilage. The sole exception is the work of Roy et al. (2004) who calculated the bending modulus (7.1 MPa) for porcine cartilage specimens using three-point bending.

Ribcage deformation, and mechanical response of the thorax in general, could be much affected by age-related changes in the costal cartilage. Calcification of the costal cartilage is used as an indicator of age and gender in forensic science (Rejtarova et al., 2004). In addition to calcification, the costal cartilage undergoes structural and compositional changes with aging, called the "amianthoid change" (Hukins et al., 1976). Altered mechanical stiffness of the costal cartilage associated with one or both of these factors (calcification, amianthoid change) could potentially result in dramatic changes in the overall pattern of deformation of the ribcage even in the absence of changes in the bone.

Mechanical testing based on indentation contact is common for both non-biological and biological material characterization. Indentation testing has been used for the development of increasingly complicated constitutive descriptions for articular cartilage, and indentation is in fact the most common technique for cartilage mechanical characterization (Mow et al., 2005). In mineralized tissues, recent studies have examined variations in responses due to local microstrucutral features such as lamellae and osteons in bone (Hoffler et al., 2000; Rho et al., 1997) and due to variations in local tissue composition (Ferguson et al., 2003). These studies demonstrate the remarkable promise of indentation testing for local measurements of mechanical behavior in non-homogeneous materials such as biological tissues.

In indentation testing, a probe that is small (relative to the size of a sample) is brought into contact with the sample to perform a localized mechanical test. Indentation tests are simple to perform, absent many of the gripping difficulties that plague tensile techniques for biomechanical characterization of hydrated soft tissues. Flat punch, (hemi-)spherical, and pointed (conical or pyramidal) indenter tip shapes are all commonly used in indentation testing, which is considered non-destructive as the sample remains largely intact following the mechanical test, unlike tensile testing to sample failure. Indentation tests are most frequently used to characterize the elastic or time-dependent deformation characteristics of a material, although aspects of failure or fracture can be considered as well. A standard indentation test consists of a single loading cycle, with a loading segment, an optional holding segment at peak load or peak displacement (depending on whether the testing is being performed in load- or displacement-control) and an unloading segment. Straightforward analytical solutions exist for the analysis of different aspects of mechanical behavior that can be probed by indentation testing, including elastic (Sneddon, 1965) plastic (Johnson, 1985; Oliver and Pharr, 1992), and viscoelastic (Johnson, 1985; Oyen, 2005).

Many studies have used load-controlled instrumented indentation to investigate the mechanical response of mineralized tissues (Rho et al., 1997; Ferguson et al., 2003), including examination of the viscoelastic response (Bembey et al., 2006). Indentation testing has also been used for material characterization of soft biological tissues in displacement-control, including the brain (Gefen et al., 2003; Miller, 2000), lung parenchyma (Lai-Fook et al., 1976), lower limb tissues (Zheng et al., 1999), and articular cartilage (Hayes and Mockros, 1971; Parsons and Black, 1977; Mak et al., 1987; Beek et al., 2003). All but one (Gefen et al., 2003) of these soft tissue indentation studies has utilized a flat-punch indenter geometry, presenting the potential complication of stress concentrations or tissue cutting at the indenter edges.

The current study includes development of a method for measurements of the mechanical behavior of costal cartilage tissue samples in displacement control using (hemi-)spherical indenter tips. The material elastic modulus and relaxation function will be obtained from each location tested via indentation. Costal cartilage of different ages will be examined, to try to ascertain any effect of age-dependence of cartilage material properties. A finite element model will be used to examine the implications of costal cartilage material property changes on deformation of the thorax.

METHODS

Materials

A standard polymeric material with known composition and material properties (PS-4 polyurethane, Vishay Measurements Group, with elastic modulus $E = 4$ MPa, and Poisson's ratio $\nu \sim 0.5$) was selected as a standard. This material is available in homogeneous sheets (thickness 3 mm) and provides a baseline linearly viscoelastic response for test development and analysis validation (Oyen, 2005).

Porcine costal cartilage tissue was obtained from young female, Yorkshire sus scrofa. (These young porcine subjects are being used as a surrogate for 6-year old humans in a different project at the Center for Applied Biomechanics [Arbogast et al., 2005].) This cartilage was visibly young, having a shiny and bluish-white appearance characteristic of healthy cartilage. Chest-plates were stored frozen and thawed prior to testing. For mechanical testing via indentation, the cartilage was cross-sectioned using a custom cutter consisting of mounted parallel scalpel blades, exposing the midsubstance of 5 mm thick sections of the tissue for indentation testing (Figure 1). Each prepared specimen was allowed to equilibrate in a physiological saline or pure water bath at room temperature (~25º C) prior to testing. Human costal cartilage tissue was obtained from rib cages of two subjects for the current preliminary report, both females aged 32 and 71. Experiments were performed primarily on cartilage from the fifth (5th) rib. Cross-sectional cartilage samples were prepared as above for the porcine cartilage and tested in a physiological saline bath at room temperature.
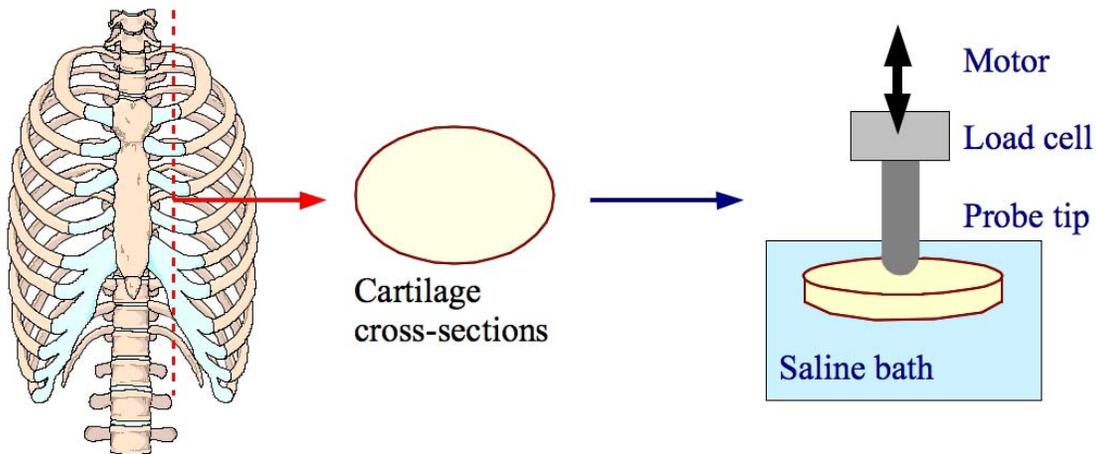

Figure 1: Schematic illustration of the costal cartilage indentation testing procedure developed in the course of the current work. Costal cartilage is sectioned and cross-sections are indented in the cartilage mid-substance using a custom sphere-tipped indentation device.

Indentation Tests

A custom, displacement-controlled indentation instrument was assembled. The driving mechanism was a custom-built linear actuator (Industrial Devices Corporation, motor model BN23, Rockford, IL.) driven by a brushless servomotor. The device was mounted vertically on a set of machinist's chucks, which allowed the device to be positioned so that the displacements were normal relative to the test specimen surface. A

100-g Microtron accelerometer (Endevco Corporation, model 7290A-100, San Juan Capistrano, CA) was mounted to the linear actuator and measured accelerations of the punch in the direction of the punch displacement. A 500-gram uniaxial load cell (Honeywell Sensotec, model 31/1435-03-04, Columbus, OH) was used in the kidney tests and a 5-pound uniaxial load cell (Honeywell Sensotec, model 31:AL311AT, Columbus, OH) was used for the rubber and costal cartilage tests. Each load cell was mounted between the linear actuator and the shaft of the spherical indenter tip. A linear potentiometer (Novotecknik, model T-25, Southborough, MA) was mounted on the actuator to verify the input displacement-time profile for the motor. A spherical indenter tip was machined from steel to a diameter of 3.15 mm.

Indenter-material contact was determined prior to each test by detection of a small (5-50 mN) load change. Pilot studies were performed using both rubber (PS-4 urethane sheet) and cross-sectioned young porcine costal cartilage. A focus of the pilot studies was to optimize the experimental parameters for testing and to establish performance characteristics of the custom indentation instrument. Optimization was performed for the two primary coefficients of a ramp-hold stress relaxation experiment: (a) the displacement rates (k) for ramping and (b) the peak displacement levels for the relaxation tests (h_{max}) (Figure 2).
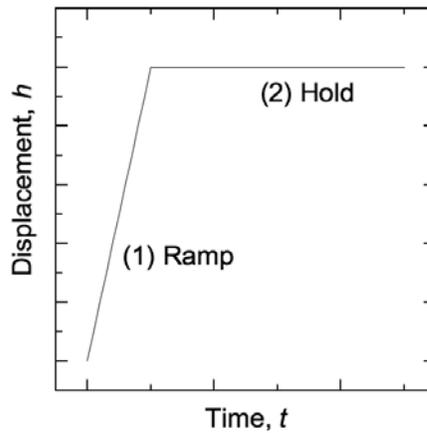

Figure 2: Indentation loading scheme for ramp-hold relaxation tests. (1) Ramp to peak displacement, h_{max}, at displacement rate k given by $k = h_{max} / t_R$ where t_R is the rise time, the time to peak displacement. (2) Peak displacement level, h_{max}, for a holding time t_{hold}.

Analytical Modeling

A novel analytical modeling technique has been developed (Mattice et al., 2006) and is summarized here. The isotropic elastic Hertzian contact (spherical indentation) expression for an incompressible material is:

$$P = \frac{4\sqrt{R}}{3} \frac{E}{(1-\nu^2)} h^{3/2} = \frac{8\sqrt{R}}{3} [2G] h^{3/2} \qquad \text{(Eqn. 1)}$$

expressed as a relationship between the extensive variables (load P, displacement h) and where R is the probe radius, E is the material elastic modulus, ν is the material Poisson's ratio, and G is the shear modulus. The relation between elastic and shear modulus values is simply $E = 3G$ for an incompressible solid ($\nu = 0.5$).

The measurement of time-dependent mechanical properties from spherical indentation tests is done via the principle of elastic-viscoelastic correspondence (Lee and Radok, 1960). Using this principle, viscoelastic operators are substituted for elastic constants in the elastic solution (Eqn. 1). This allows for the measurement of an elastic modulus (zero-time shear modulus) and an arbitrary relaxation function (common forms include the sum of exponentials or the Prony series) within the experimental time-frame of interest without making *a priori* restrictions on the precise details of the material behavior (viscoelastic vs. poroelastic). The analysis for elastic-viscoelastic correspondence can be based on a differential operator method (Cheng et al., 2005) or a Boltzmann hereditary integral method (Oyen, 2005). This technique has

been utilized for characterization of polymers under indentation creep conditions (Cheng et al., 2005; Oyen, 2005).

For a step-load relaxation experiment, the relaxation response can be simply expressed as (Johnson ,1985):

$$P(t) = \frac{8\sqrt{R}}{3} h_0^{3/2} [2G(t)] \tag{Eqn. 2}$$

where $G(t)$ is the shear relaxation modulus. However, for real experiments, a step-displacement assumption is inadequate and ramping time ("rise time", t_R) must be directly considered in the analysis. A Boltzmann integral method will be used here for displacement-controlled ramp relaxation, directly paralleling the construction considered previously for load-controlled spherical indentation (Oyen, 2005). The experimental conditions for ramp-hold relaxation experiments in displacement control are:

$$h(t) = kt, 0 \leq t \leq t_R$$
$$h(t) = kt_R = h_{max}, t \geq t_R \tag{Eqn. 3}$$

These displacing conditions can be inserted into the generalized Boltzmann integral expression for spherical indentation under displacement control, assuming incompressibility ($\nu = 0.5$):

$$P(t) = \frac{8\sqrt{R}}{3} \int_0^t G(t-u) \left[\frac{d}{du} h^{3/2}(u) \right] du \tag{Eqn. 4}$$

For displacement control, the integral for constant displacement-rate loading has no analytical solution and must be solved numerically (Sakai, 2002). However, in load control, a creep-displacement-time analytical solution can be determined by direct integration. In previous work (Oyen, 2005), the solution for load-controlled creep was expressed as the step-loading creep solution with compliance parameters adjusted by a "ramp correction factor." For displacement-controlled relaxation, a similar approach can be taken, incorporating a ramp-modification to the step displacement relaxation solution. For a material relaxation function of the form:

$$G(t) = C_0 + C_1 \exp(-t/\tau_1) + C_2 \exp(-t/\tau_2) + C_3 \exp(-t/\tau_3) \tag{Eqn. 5}$$

the load-relaxation solution has the form:

$$P(t) = B_0 + B_1 \exp(-t/\tau_1) + B_2 \exp(-t/\tau_2) + B_3 \exp(-t/\tau_3) \tag{Eqn. 6}$$

This form results from the numerical integration of Eqn. 4 for the conditions given by Eqn. 3. This function can be fit directly to the experimental load-time relaxation data (during the holding segment $h(t) = h_{max}$). The fitting parameters (B_k) can be related to the material parameters (C_k) via the experimental controllables (h_{max}, t_R, R) via:

$$C_0 = \frac{B_0}{h_{max}^{3/2} (8\sqrt{R}/3)} \tag{Eqn. 7}$$

$$C_k = \frac{B_k}{(RCF_k) h_{max}^{3/2} (8\sqrt{R}/3)}, \quad k = 1,2,3 \tag{Eqn. 8}$$

where

$$RCF_k = \frac{\tau_k}{t_R} \left[\exp\left(\frac{t_R}{\tau_k}\right) - 1 \right], \quad k = 1,2,3 \tag{Eqn. 9}$$

and *RCF* is the "ramp correction factor," the difference between the observed values for analysis assuming ramp loading vs. the step loading assumption (Oyen, 2005).

From the obtained relaxation moduli, the instantaneous shear modulus (G_0) and long time (G_∞) shear modulus values can be computed:

$$G_0 = G(0) = \frac{C_0 + C_1 + C_2}{2}$$

$$G_\infty = G(\infty) = \frac{C_0}{2}$$

(Eqn. 10)

From these values, the instantaneous and long-time elastic modulus values (E_0 and E_∞) can be computed, recalling that for an incompressible solid $E = 3G$.

Finite Element Modeling

A finite element model of an isolated rib "hoop" including rib bone, sternum, vertebral body, costo-vertebral joint ligaments and costal cartilage was generated at fifth rib level using Thums Occupant (50th percentile American male) which was developed by Toyota Central R&D Labs, Inc.

The costal cartilage was modeled as elastic shells and solids respectively for representing the perichondrium surface layer and the cartilage matrix. The vertebral body was modeled as a rigid body, and other bones were modeled as elastic-plastic shells and elastic solids respectively for cortical and trabecular bones. The rib bone is connected to the vertebral body with several elastic bars as costo-vertebral joint ligaments. Young's modulus of costal cartilage was considered as 10 MPa (soft case) or 1 GPa (stiff case) and each perichondrium modulus was set as twice as stiff as that of the corresponding matrix. Table 1 shows the material properties used in deformable parts of the model.

The vertebral body was held fixed. The steering-wheel sized hub load was applied with a 0.15 m diameter rigid cylinder to the mid-sternum in the anterior-posterior direction with 1 m/s of constant velocity up to 37.5 mm of hub displacement (17.5 % of initial distance between sternum and vertebra). The velocity is considered as a rate similar to that experienced by restrained PMHS in 48 km/h frontal sled tests (Kent et al., 2004).

RESULTS

Rubber indentation-relaxation tests were performed in triplicate at a peak displacement level (h_{max}) of 0.3 mm and a fixed rise time (t_R) of 1.6 seconds. The force-time (*P-t*) data for the three experiments were averaged for analysis. The experimental data are presented in Figure 3 as hollow symbols and the solid line represents the model fit. The numerical value of the shear modulus (G_0) was found to be 1.21 MPa, in reasonable agreement with the known value (from the manufacturer) of $G = 1.33$ MPa.

Table 1. Finite element model parameters.

Tissue		Material/Element Type	Young's Modulus, E (MPa)	Poisson's ratio, ν	Yield Stress, σ_0 (MPa)	Density, ρ (kg m^{-3})	Thickness, t (m)
Costal cartilage (soft case)	Perichondrium	Elastic shell	20	0.4	–	1500	0.001
	Matrix	Elastic solid	10	0.4	–	1500	–
Costal cartilage (stiff case)	Perichondrium	Elastic shell	2000	0.4	–	1500	0.001
	Matrix	Elastic solid	1000	0.4	–	1500	–
Rib bone and sternum	Cortical	Elastic-plastic shell	11500	0.3	70*	2000	0.0007
	Trabecular	Elastic solid	40	0.45	–	862	–
Costo-vertebral joint	Radiate lig.	Elastic bar	10	0	–	1000	–
	Anterior costo-tansverse lig.						
	Lig. of the tubercle						
	Lig. of the neck						

* Plastic tangent modulus of cortical bone shell: 2156.3 MPa.
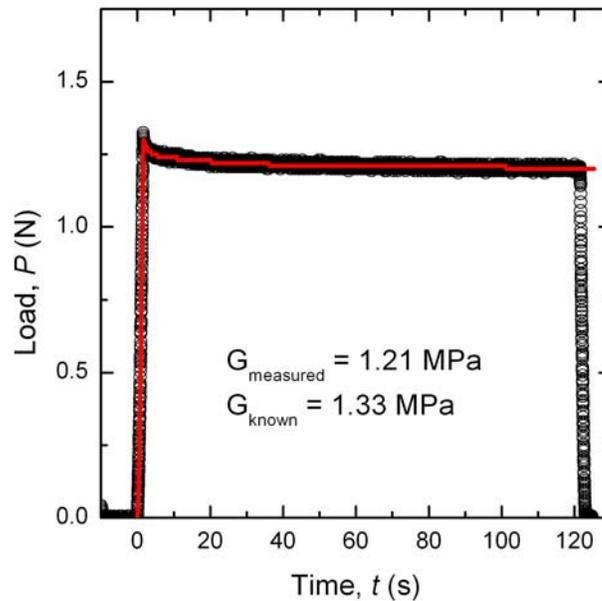

Figure 3: Experimental indentation load-time (*P-t*) relaxation data (grey symbols) for PS-4 rubber polymer standard material tested at peak displacement (h_{max}) of 0.3 mm. The solid line is numerical ramp-hold response based on the exponential fit to the relaxation data (Eqns 4,6-9).

Porcine cartilage indentation tests were next performed to 0.4 mm peak displacement with a rise time of 2.1 seconds. Tests were performed on cartilage samples from the same rib section when one portion of the cartilage had been soaked to equilibrate in physiological saline and the other had equilibrated in water. This condition presents an opportunity to test an expected experimental result, that cartilage soaked in water would be stiffer than that soaked in saline due to proteoglycan swelling.

The raw load-time relaxation responses are shown in Figure 4 for cartilage tested in physiological saline (0.9 % NaCl) and in water. The solid lines are the model-fits to the experimental data. The apparent tissue stiffness (both G_0 and G_∞) has been dramatically increased in the water-soaked condition, in agreement with the expected outcome of the experiment. The shape of the relaxation function has not changed dramatically (Figure 5, top), merely the scaling as evidenced by the stiffness values (Figure 5, bottom).

Raw load-time relaxation responses are shown in Figure 6 for old and young human costal cartilage in saline. The solid lines are the model-fits to the experimental data. In the small pool of experiments conducted to date, no obvious trend has emerged for the differences between older and younger human costal cartilage but studies are ongoing.
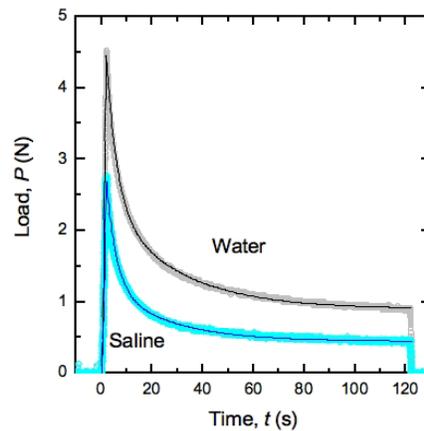

Figure 4: Indentation relaxation load-time (*P-t*) plots for two porcine cartilage from the same rib sample, but soaked in either water or physiological saline (0.9% NaCl). The hollow points are the experimental data and the solid lines are the model fits as described above.
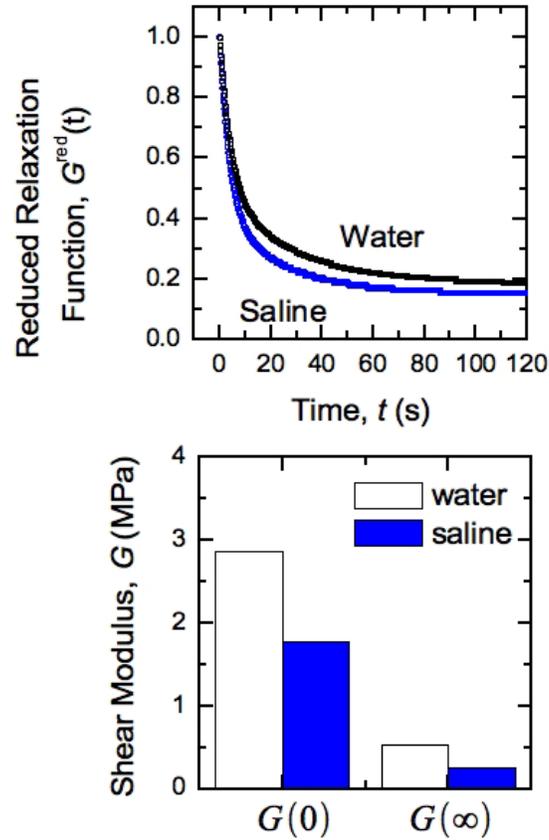
Figure 5: (top) Reduced relaxation functions {$G(t)/G(0)$-t} for porcine tissue soaked in water and in physiological saline (data from Figure 4). (bottom) Time zero and long-time shear modulus values (G_0, G_∞) for water- and saline-soaked young porcine cartilage.
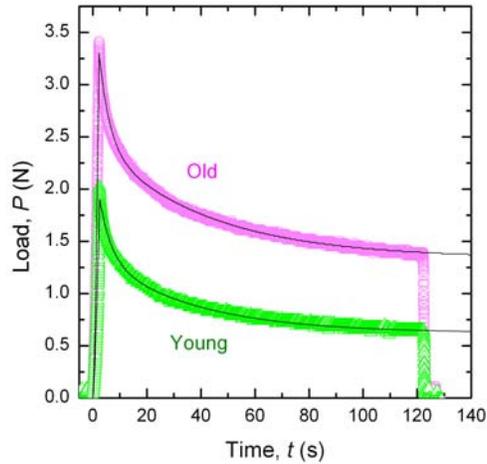

Figure 6: Experimental indentation load-time (P-t) relaxation data (grey symbols) for human costal cartilage tested at peak displacement (h_{max}) of 0.5 mm. The solid line is numerical ramp-hold response based on the exponential fit to the relaxation data (Eqns 4,6-9).

The implications for costal cartilage property changes are seen in the results presented in Figures 7 and 8. A finite element model of a portion of the ribcage is examined, with comparisons for two different values of the costal cartilage modulus (compliant, 10 MPa, and stiff, 1 GPa). Figure 7 shows the curves of anterior fifth ribcage load versus the mid-sternum deflection. The anterior fifth ribcage load is calculated as a contact reaction force between the steering-wheel sized hub and the fifth ribcage. The mid-sternum deflection is the ratio of the hub displacement to the initial distance between sternum and vertebra. The dashed line shows the approximate stiffness, compared to the solid curve demonstrating the model response. The stiffness of fifth ribcage with stiff cartilage (2056 N) was twice as large as that with soft cartilage (999.8 N). The von Mises stress distributions for the two cases are shown in Figure 8, for 37.5 mm of hub displacement on the shell surfaces (17.5 % of initial distance between sternum and vertebra). The maximum stress was 85 MPa for the compliant case (left) and 100 MPa for the stiff case (right), 1.2 times as large as that for the compliant case. In both cases, the stress localization starts near the costo-chondral region and around the tubercle region. However the costo-chondral region deforms more in the soft case, while the costo-vertebral joint rotates more in the stiff case.

These results imply that changes in the costal cartilage modulus could change the whole thorax stiffness in frontal impact. The stiffer cartilage could induce larger stress in the bone than the soft cartilage could. On the other hand, the compliant cartilage could result in increased deformation of the internal organs more locally via the pleura under the costo-chondral region. Thus, the material property change in costal cartilage could affect not only the deformation pattern but also the subsequent injury pattern.
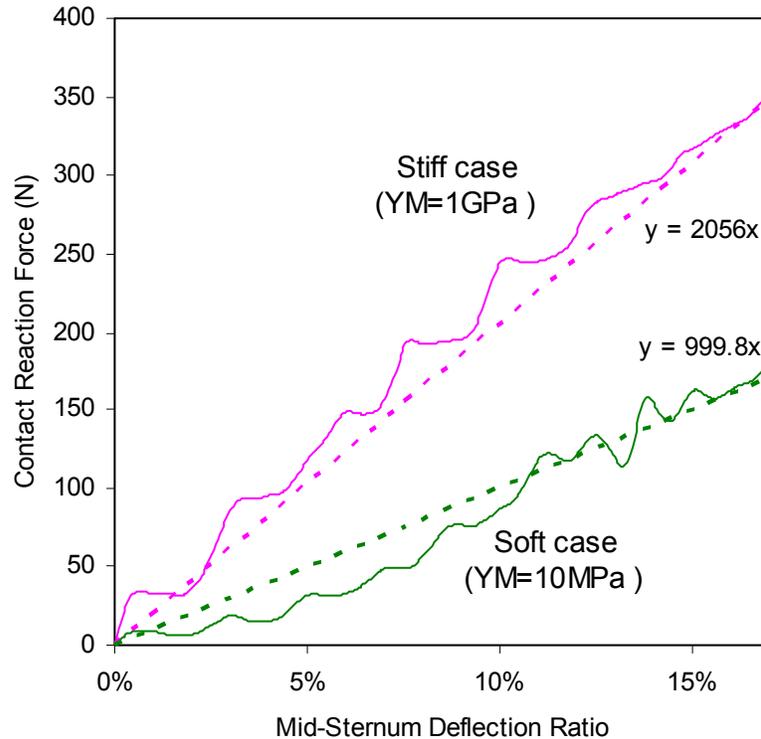

Figure 7: Curves of anterior fifth ribcage load versus mid-sternum deflection calculated with the finite element model for costal cartilage modulus of 10 MPa or 1 GPa.
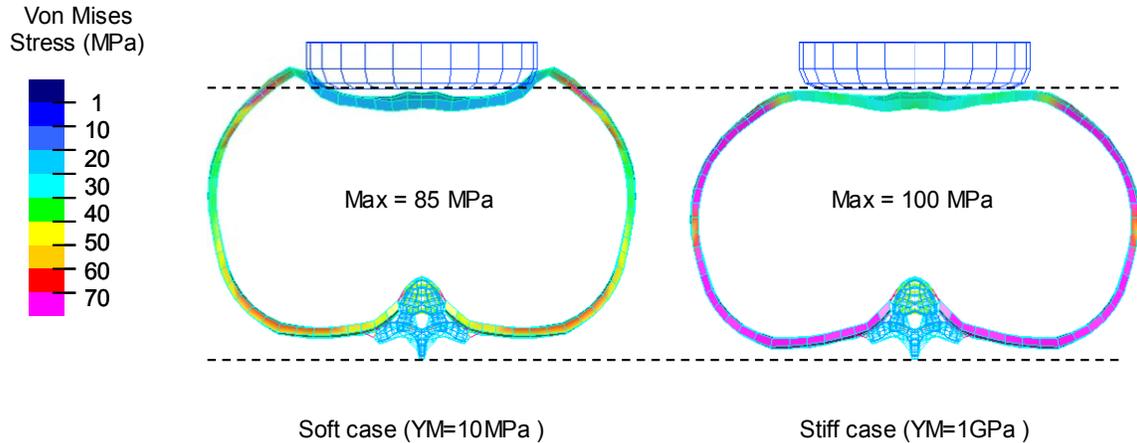
Figure 8: Comparison of the deformed mesh and von Mises stress contours for finite element model of the fifth rib for costal cartilage modulus of 10 MPa (left) or 1 GPa (right).

CONCLUSIONS

In summary, an indentation method has been developed and applied to the measurement of effective elastic and time-dependent mechanical properties of the ribcage costal cartilage. Ongoing work will involve characterization of the costal cartilage of subjects of different ages to quantify the alterations in costal cartilage with aging. The implications of costal cartilage modulus changes were explored with a finite element model, and it was found that a material property change in costal cartilage could affect not only the deformation pattern but also the injury pattern.

ACKNOWLEDGEMENTS

REFERENCES

ARBOGAST, K., MARIGOWDA, S., KENT, R., STACEY, S., MATTICE, J., TANJI, H., HIGUCHI, K., and ROUHANA, S. (2005). Evaluating pediatric abdominal injuries. Proc. 19th Conference on the Enhanced Safety of Vehicles, Washington DC.

BEEK, M., KOOLSTRA, J., and VAN EIJDEN, T. (2003). Human temporomadibular joint disc cartilage as a poroelastic material. Clinical Biomechanics, 18, 69.

BEMBEY, A. K., OYEN, M. L., BUSHBY, A. J., and BOYDE, A. (2006). Viscoelastic properties of bone as a function of hydration state determined by nanoindentation. Philosophical Magazine (submitted).

CHENG, L., XIA, X., SCRIVEN, L. E., and GERBERICH, W. W. (2005). Spherical-tip indentation of viscoelastic material. Mechanics of Materials, 37, 213-226.

FERGUSON, V. L., BUSHBY, A. J., and BOYDE, A. (2003). Nanomechanical properties and mineral concentration in articular calcified cartilage and subchondral bone. J. Anat, 203, 191-202.

GEFEN, N., ZHU, Q., RAGHUPATHI, R., and MARGULIES, D. S. (2003). Age-dependent changes in material properties of the brain and braincase of the rat. J. Neurotrauma, 20, 1163-77 .

HAYES, W. C. and MOCKROS, L. F. (1971). Viscoelastic properties of human articular cartilage. J. Appl. Physiol., 31, 562-8.

HAYES, W. C., KEER, L. M., HERRMANN, G., and MOCKROS, L. F. (1972). A mathematical analysis for indentation tests of articular cartilage. J Biomech, 5, 541-51.

HOFFLER, C. E., MOORE, K. E., KOZLOFF, K, ZYSSET, P. K., and GOLDSTEIN, S. A. (2000). Age, gender, and bone lamellae elastic moduli. J Orthop Res. May;18, 432-7.

HUKINS, D. W., KNIGHT, D. P., and WOODHEAD-GALLOWAY, J. (1976). Amianthoid change: orientation of normal collagen fibrils during aging. Science. 1976 Nov 5;194 (4265):622-4.

JOHNSON, K. L. (1985). Contact Mechanics. UK: Cambridge University Press.

KEMPER, A. R., MCNALLY, C., KENNEDY, E. A., MANOOGIAN, S. J., RATH, A. L., NG, T. P., STITZEL, J. D., SMITH, E. P., DUMA, S. M., and MATSUOKA, F. (2005). Material properties of human rib cortical bone from dynamic tension coupon testing. Stapp Car Crash Journal, 49:199-230.

KENT, R., LESSLEY, D., and SHERWOOD, C. (2004). Thoracic response corridors for diagonal belt, distributed, four-point belt, and hub loading. Stapp Car Crash Journal, 48:495-519.

KENT, R., HENARY, B., and MATSUOKA, F. (2005a). On the fatal crash experience of older drivers. 49th Annual Meeting Proceedings, AAAM, 371-391.

KENT, R., LEE, S., DARVISH, K., WANG, S., POSTER, C., LANGE, A., BREDE, C., LANGE, D., and MATSUOKA, F. (2005b). Structural and material changes in the aging thorax and their role in reduced thoracic injury tolerance. Stapp Car Crash Journal , 49:231-249.

LAI-FOOK, S., WILSON, T., HYATT, R., and RODARTE, J. (1976). Elastic constants of inflated lobes of dog lungs. J. Appl. Physiol., 40, 508-13.

LEE, E. H. and RADOK, J. R. M., (1960). Contact problem for viscoelastic bodies, Journal of Applied Mechanics, 27, 438-44 .

MAK, W., LAI, D. V., and MOW, V. C. (1987). Biphasic indentation of articular cartilage – I.Theoretical analysis. J. Biomechanics, 20, 703-14.

MALLINGER, R. and STOCKINGER, L (1988). Amianthoid (asbestoid) transformation: electron microscopical studies on aging human costal cartilage. Am J Anat., 181, 23-32.

MATTICE, J. M., LAU, A. G., OYEN, M. L., and KENT, R. W. (2006). Spherical Indentation Load-Relaxation of Soft Biological Tissues. Journal of Materials Research (in press).

MILLER, K. (2000). Constitutive modeling of abdominal organs. *J. Biomechanics,* 33, 367-73.

MOW, V. C., GU, W. Y., and CHEN, F. H. (2005). Structure and function of articular cartilage and meniscus. (chapter 5) Basic Orthopaedic Biomechanics and Mechanobiology, third edition, Mow VC and Huiskes R, eds. Philadelphia: Lippincott, Williams and Wilkins.

OYEN, M. L. (2005). Spherical Indentation Creep Following Ramp Loading. J. Mater. Res., 20(8):2094-2100.

OLIVER, W. C. and PHARR, G. M. (1992). Improved technique for determining hardness and elastic modulus using load and displacement sensing indentation experiments. J Mater Res, 7(6):1564-83.

PARSONS, J. and BLACK, J. (1977). The viscoelastic shear behavior of normal rabbit articular cartilage. J. Biomechanics, 10, 21-9.

PATTIMORE, D., THOMAS, P., and DAVE, S. (1992). Torso injury patterns and mechanisms in car crashes: an additional diagnostic tool. Injury: The British Journal of Accident Surgery 23, 123-126.

REJTAROVA, O., SLIZOVA, D., SMORANC, P., REJTAR, P., and BUKAC, J. (2004). Costal cartilages - a clue for determination of sex. Biomed Pap Med Fac Univ Palacky Olomouc Czech Repub. 148, 241-3.

RHO, J-Y., TSUI, T.Y., and PHARR, G. M. (1997). Elastic properties of human cortical and trabecular lamellar bone measured by nanoindentation. Biomaterials 18, 1325-1330.

ROSENBERG, L., JOHNSON, B., and SCHUBERT, M. (1965). Proteinpolysaccharides from human articular and costal cartilage. J Clin Invest. 44, 1647-56.

ROY, R., KOHLES, S. S., ZAPOROJAN, V., PERETTI, G. M., RANDOLPH, M. A., XU, J., and BONASSAR, L. J. (2004). Analysis of bending behavior of native and engineered auricular and costal cartilage. J Biomed Mater Res A. 68, 597-602.

SAKAI, M. (2002). Time-dependent viscoelastic relation between load and penetration for an axisymmetric indenter. Philosophical Magazine A., 82(10), 1841-9.

SNEDDON, I. N. (1965). The relation between load and penetration in the axisymmetric Boussinesq problem for a punch of arbitrary profile, Int. J. Engng. Sci. 3, 47-57.

STITZEL, J. D., CORMIER, J. M., BARRETTA, J. T., KENNEDY, E. A., SMITH, E. P., RATH, A. L., DUMA, S. M., and MATSUOKA, F. (2003). Defining regional variation in the material properties of human rib cortical bone and its effect on fracture prediction. Stapp Car Crash Journal, 47:243-65.

ZHENG, Y., MAK, A. F., and LUE, B. (1999). Objective assessment of limb tissue elasticity: development of a manual indentation procedure. J. Rehabil. Res. Dev., 36(2), 71-85.

DISCUSSION

PAPER: **Mechanical Characterization of Costal Cartilage**

PRESENTER: ***Michelle L. Oyen, University of Virginia Center for Applied Biomechanics and Nissan Motor Company***

QUESTION: *Erik Takhounts, NHSTA*
I have a couple of questions for you with regard to your material modeling. One of them is how you deal—It looks to me if you would like to extrapolate, represent one material across all ages, you are going to have to deal with spatial and temporal nonlinearities looking at your stress relaxation data and reduced relaxation function. So, is that what you're going—planning to do? That's question #1. Question #2: Your primary model deformation is bending, I think, on the cartilage when it's been loaded and your testing material is basically in compression. Are you assuming that you can calculate what the total stiffness matrix is going to be on the cartilage or you assume it's homogeneous and isotropic?

ANSWER: Okay. So, one of the advantages of this sort of a technique is we're not actually putting terribly much information into as a material model. We're measuring as stiffness and measuring as time-dependant. But in order to establish if the tissue is or is not nonlinear, which articular cartilage under compression frequently isn't, we need to do a lot more tests and we need to do tests at different levels and show that it actually is or is not behaving nonlinearly and then to also look at how that may or may not be changing as a function of the changes that we do see. Another advantage of an indentation test is that you get much less anisotropy than you get in a tensile test, say, because the stress field is much more complicated. And so, you actually do sample different types of loading and different loading directions. And so, it gives you a good, sort of first-hand measure of the stiffness in that region. And so I think that in order to move on to validate full models of the whole ribcage, perhaps there will be additional tensile tests or other types of loading that you would want to look it. But to get a first order of approximation, this is actually a really good technique for doing so.

Q: The reduced relaxation function that you show in one of the graphs is just from one test?

A: Correct.

Q: You just presume that you are going to use quasilinear viscoelastic model?

A: No! I'm going to to presume I'm not going to use quasilinear viscoelastic model—

Q: Why did you use a quasi?

A: Because the data shows that I have to have one. So if I make measurements in a layer of cartilage at a bunch of different displacement levels, then I get a different reduced relaxation function. Then yes, that would indicate that I should go to KLB model. But again for cartilage and compression, that's not necessarily going to be the case.

Q: Alright. How are you going to deal with homogenic and isotropic?

A: Well as I said, the indentation test does, in fact, produce the overall level of anisotropy. So if you have a modulus value versus orientation that's a quite steep change—maybe a factor of two change, in indentation you may expect to see about half that change. And, you can actually measure it and there are analytical solutions for anisotropic indentation where you do take—You can take a cube of material, measure in different directions and you actually can then back out from your contact conditions the actual anisotropic effect of stiffness coefficients, CIJs. And if you're interested, I can show you papers where that's done. Obviously we haven't looked at that yet in this case.

Q: Alright. Thank you.

Q: *Guy Nusholtz, Daimler Chrysler*
Did you look at different orientations on your indentation when you did it?

A: Not yet. Not yet. As I said, this is very preliminary, new work and ongoing, and there's a lot more to be done experimentally.

Q: Okay. It'll be interesting to see what type of variations you get.

A: Absolutely! Absolutely! And you know, there's interesting competing factors here. You have the potential structural changes with aging that could make the tissue anisotropic because of the collagen becoming more oriented. But also then once you start mineralizing that, it may actually act in the other direction to go back to being less anisotropic depending on how the mineral actually lies down, which, you know, until we do more experiments, we won't have very much of an idea of that.

Q: So once you get your experimental procedure, you can try all different ways and figure out the scanner.

A: Correct.

Q: And then solve all the problems in the world!

Q: *Stewart Wang, University of Michigan*
It's very nice work. Clinically, we certainly see these changes with aging in the costal cartilage, and we have also looked at five or six hundred chest CTs and we noticed a large amount of variability in terms of various properties, such as, which might be calcification. Have you done the studies to look at the CT of these samples or are you considering doing CTs and micro-CTs on these?

A: Yes. In fact, one of the Masters students in our lab did just do a series of CTs studies and we will be looking at that, as well as with these kind of indentation experiments, you can go in and make measurements of the mineral more locally and try to get a feel for how changes in mineralization are resulting in changes in moduluses because, of course, that's not a linear affect.